Eur. Phys. J. B **17**, 713–722 (2000)

THE EUROPEAN PHYSICAL JOURNAL B

EDP Sciences

Tracer diffusion and correlations in ordered adsorption systems with defect-controlled transport mechanisms

A.A. Chumak[1] and C. Uebing[2,3,a]

[1] Institute of Physics of the National Academy of Sciences, pr.Nauki 46, 252028, Kiev, Ukraine
[2] Max-Planck-Institut für Eisenforschung, 40074 Düsseldorf, Germany
[3] Lehrstuhl für Physikalische Chemie II, Universität Dortmund, 44227 Dortmund, Germany

Received 20 September 1999 and Received in final form 14 April 2000

Abstract. In this study we develop a theory of tracer diffusion in 2D lattice-gas systems with strongly repulsive nearest neighbor interactions. The study is performed for a square lattice in the vicinity of half monolayer coverage. In this case the lattice gas forms a highly-ordered c(2×2) phase. The adatom kinetics is reduced to the problem of random walks of long-living structural defects. The correlated motion of tracer-defect pairs is considered. Equations for correlation functions of tracer-vacancy, tracer-excessive adatoms and tracer-dimer pairs are derived and solved in terms of microscopic jump probabilities of defects. The solutions are exact in the case of dominant single defect transport mechanisms. In the case of dimer transport we applied the approximation of short-range correlation length. The values obtained for the correlation factor are in good agreement with the results of computer simulations in the over-stoichiometric range, while for sub-stoichiometric coverages the agreement is not very good.

PACS. 82.20.Mj Nonequilibrium kinetics – 68.35.Fx Diffusion; interface formation – 64.60.Cn Order–disorder transformations; statistical mechanics of model systems

1 Introduction

First- or second-order phase transitions change the symmetry of an adatom system. At high temperatures the system is disordered and the description of its macroscopic state requires the knowledge of the adatom concentration only. In this case, there exists a well defined diffusion coefficient describing the decay of long-scale inhomogeneities of the adatom density. As the temperature is lowered, the initially uniform adatom distribution is transformed into a mixture of phases with different densities (phase transition of first order) or into an ordered structure (or domains of ordered structures) with the period larger than the lattice constant (phase transition of second order). It is evident that two (or more) different diffusion coefficients appear in the first case. Each diffusion coefficient describes adatom flows in a given phase (intraphase diffusion coefficient). However, it is not clear how to describe the diffusion in a macroscopically large system, which is a random mixture of different phases. Computer simulations in this case constitute a severe problem because huge lattice sizes are required to observe the characteristic many-domain structures. If only a small number of domains are present, their evolution is strongly affected by the boundary conditions and differs from the evolution in an infinite system. To our knowledge there is no rigorous theory connecting the intraphase diffusivities with the computer simulation data in such a complex system.

The case of the second order phase transition is more convenient for both theoretical studies and Monte Carlo (MC) simulations. In this case, as already mentioned, the system exhibits ordering at low temperatures, *i.e.* the whole lattice decomposes into sublattices with different average occupation numbers. Perfect ordering at $T = 0$ and characteristic (stoichiometric) total coverages (which depend on the symmetry of the lattice) corresponds to the situation where some of the sublattices are completely filled while others remain empty. Intuitively, it seems to be a reasonable physical picture when the excessive adatom concentration (adatom inhomogeneity) is redistributed between different sublattices. The state of local equilibrium is established between different sublattices if the inhomogeneities are sufficiently smooth and small. The disturbance of the adatom density causes local disturbances of the occupation numbers in each sublattice (coupled disturbances). The complexes formed by such disturbancies evolve in accordance with the ordinary diffusion equation and, therefore, an appropriate theory for the description of diffusion in such a system can be easily developed, as is shown in the remainder of this paper.

At the same time, computer modelling of highly ordered states involves considerable difficulties. First of all,

[a] e-mail: uebing@mpie.de

ordering freezes adatom motion, and this results in an increase of computer time required to ensure reliable statistics. Besides that, special precautions should be taken during Monte Carlo simulations in order to avoid uncontrolled effects of antiphase domain walls or other macroscopic defects (see for example [1]). In view of this point, rigorous theoretical descriptions provide possibilities to test computer algorithms and thus could be of enormous importance.

The theoretical study of the low-temperature phase is very simple in the case of highly-ordered states which are established in the vicinity of the stoichiometric coverage. This specific situation was analyzed in our previous paper [2], where the theory of adatom diffusion on a square lattice with nearest neighbor (NN) repulsive interactions between adatoms was developed. This system exhibits c(2×2) or $(\sqrt{2} \times \sqrt{2})$R45° ordering at low temperatures and half coverage. The ideal ordering can be described by two interpenetrating square sublattices whose unit cells are rotated by 45° and its base vectors are expanded by $\sqrt{2}$ with respect to the primitive unit cell of the underlying square lattice. It follows from the theory that in the case of half coverage the total number of defects (vacancies in the filled sublattice and excessive atoms in the almost empty sublattice) exponentially decreases if the interaction parameter increases (or if the temperature decreases). A very small number of defects can also be seen visually in snapshots obtained by means of MC simulation [3]. The snapshots exhibit an almost ideal adatom arrangement at half coverage. Hence, the problem of adatom diffusion reduces to the problem of random walks in a rarefied gas of defects (nearly ideal gas). We managed to obtain analytical formulas for the jump diffusion coefficient (adatom mobility) and the chemical diffusion coefficient (the coefficient defined by Fick's law) in [2,4]. Our equations represent the exact solution of the problem in the limiting case when the deviation of the adatom coverage from stoichiometry is small while the interaction parameter is large. The obtained results considerably differ from those following from the earlier theories [5,6] based on uncorrelated adparticle motion.

In addition, expressions for the tracer diffusion coefficient D^* were derived in [2]. Qualitatively, the behavior of D^* is similar to that of the jump diffusion coefficient D_j and our studies [2,4] provide evidence supporting this point. The ratio $r \equiv D^*/D_\mathrm{j}$ contains valuable information on both the adatom transport mechanism and the correlations between successive tracer jumps (see for example [1,7]). The correlation effects show the existence of the memory of the system. Correlation effects belong to those physical phenomena whose theoretical study requires special care. In what follows, we show that a sufficient accuracy in the theoretical description of r (or D^*) can be obtained only beyond the approximation of uncorrelated tracer-defect jumps which was implicitly employed in [2,4]. Hence, the purpose of the present work is to develop a theory of tracer diffusion based on the model of adatom migration through defect transport mechanism considering tracer-defect correlations. This paper complements our previous study with a more accurate solution of the tracer diffusion problem.

2 Migration of defects

In order to obtain the diffusion coefficients, we have to specify the microscopic mechanism of adatom jumps. As before, we assume that adatom jumps occur between NN lattice sites. The jump frequency is given by

$$\nu_{ik} = \nu_0 \exp[\varepsilon_i],$$

where $\nu_0 = \text{const}$. ε_i is the total interaction energy of the moving adatom at its initial site i and its nearest neighbors, *i.e.*

$$\varepsilon_i = \sum_{NN} \varphi n_j.$$

φ is the dimensionless adatom-adatom interaction parameter ($\varphi \gg 1$) and $n_j = 0, 1$ is the occupation number of the jth NN site.

The strong dependence of the jump frequency on the number of NN adatoms allows the problem of adatom diffusion to be reduced to the problem of defect migration only. In the following we will explain that some types of adatom jumps do not contribute to the hydrodynamic mass flow. Figure 1a illustrates this point. The adatom displacement from site 1 to site 2 (adatom jump from the filled sublattice to the empty one) results in the formation of a short-lived state. Three NN adatoms "push out" the adatom from site 2 to its former position 1 almost immediately (the occupation time of site 2 is of the order of ${\nu_0}^{-1}\mathrm{e}^{-3\varphi}$). As we see, the adatom arrangement is not changed after this pair of strongly correlated jumps. On the other hand, jumps of this type, though being useless in the macroscopic mass flow, are of great importance in establishing the equilibrium defect concentrations. The first jump from site 1 to site 2 may become the initial step of a defect-pair generation event (with the probability $7\mathrm{e}^{-3\varphi}$), which includes three successive jumps. The theory of generation-recombination processes was developed and discussed in detail in [2].

Figure 1b illustrates the adatom configuration with an excessive particle in the empty sublattice (in site 0). This adatom can jump to site 1 with the probability 1/2 almost immediately after site 1 becomes available, for instance after the present occupant of site 1 has moved to site 2. As a result, the structural defect ("black defect" in the terminology introduced in [2,4]) migrates from site 0 to site 2. It was shown that this type of defect which jumps to the NNN site in the empty sublattice has a characteristic frequency equal to $\gamma_b(2a) = \nu_0\mathrm{e}^{\varphi}/2$. The frequency of black defect jumps to NN sites (for example, from site 0 to site 3) is twice as high, $\gamma_b(\sqrt{2}a) = 2\gamma_b(2a)$. In contrast to the case shown in Figure 1a, black defect jumps result in the displacements of two different adatoms in the same direction (or in perpendicular directions), and thus black defects can be considered as the quasiparticles contributing to macroscopic mass transport.

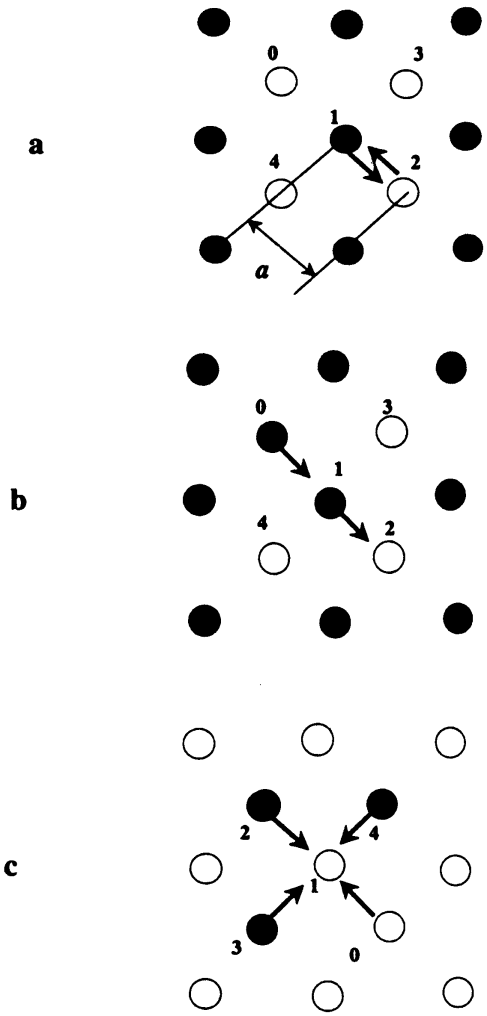

Fig. 1. Square lattice of adsorption sites. For low temperatures the lattice can be divided in two interpenetrating sublattices of empty (open circles) and filled (black circles) sites. (a) Two strongly correlated successive jumps $1 \rightarrow 2$ and $2 \rightarrow 1$ give no contribution in the mass transport. (b) Filled site 0 of the empty sublattice forms a black defect. (c) Empty site 0 of the filled sublattice forms a white defect. Displacements of both defect species contribute in the mass transport.

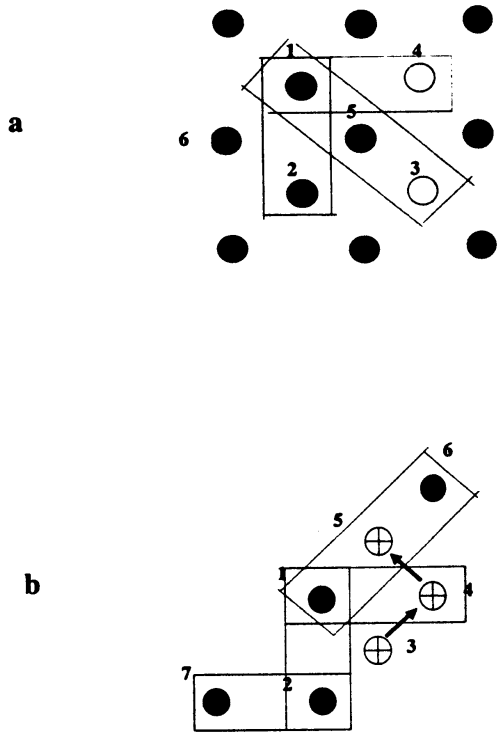

Fig. 2. Illustration of dimer motion. (a) Two black defects at sites 1 and 2 form a nearest-neighbor (NN) black dimer. As the adatom jumps from site 5 to sites 4 or 3, the dimer can be transformed either into a similar nearest-neighbor dimer 1-4 or into a next-nearest-neighbor (NNN) dimer 1-3. (b) Illustration of tracer-dimer concerted motion. Initially, the dimer and the tracer are at sites 1-2 and 3, respectively. Two successive dimer jumps to sites 1-4 and 1-6 displace the tracer to sites 4 and 5. The dimer jump from 1-2 to 7-2 position leaves the tracer in the initial site 3. Only a few lattice sites "visited" by dimer or tracer are shown.

Figure 1c illustrates the process of vacancy (white defect) displacement from site 0 to sites 2, 3, 4. This process consists of two strongly correlated successive jumps of the same adatom which occupies one of the sites 2, 3 or 4 in the initial state. The probabilities of vacancy jumps obtained in [2] and [4] are equal to $\gamma(2a) \equiv \frac{1}{2}\nu_0$ and $\gamma(\sqrt{2}a) = 2\gamma(2a)$ for jumps to NNN (site 2, Fig. 1c) and to NN (sites 3, 4, Fig. 1c) sites, respectively. The vacancy mobility is by an exponential factor e^{φ} lower than the black defect mobility.

Along with the simplest elementary displacements caused by single defect jumps, we have also dealt with the motion of dimer configurations of defects in [2]. Figure 2a shows the case of two NN black defects (NN dimer). Initially, the defects in sites 1 and 2 form a NN dimer in the empty sublattice. It can be easily seen that the adatoms in sites 5 and 6 have very high jump probabilities (equal to $\nu_0\mathrm{e}^{2\varphi}$). An adatom jump from *e.g.* site 5 to site 3 or 4 is almost immediately followed by a jump of one of the adatoms in sites 1 or 2 to the then free site 5. As a consequence, the black dimer migrates either to the sites 1 and 4 (to form a NN dimer) or to the sites 1 and 3 (to form a NNN dimer). The probability of dimer jumps per unit time interval is equal to $\Gamma = \frac{1}{3}\nu_0\mathrm{e}^{2\varphi}$ (see [2]). The simplest geometric consideration shows that the black dimer behaves like a long-lived quasiparticle. It undergoes many rotations and transformations from NN to NNN species before disintegration. It is clear, that the average number of dimers in the highly-ordered state is much lower than the number of single defects. On the other hand, the dimer mobility is much higher than the mobility of a black defect ($\Gamma/\gamma_b \propto \mathrm{e}^{\varphi} \gg 1$). For this reason, the dimer contribution can dominate the adatom diffusion (see [2]). It might seem that in this case we must take into account trimer configurations too. Trimers are present at a low concentration and possess a very high jump probability which is of the order of $\nu_0\mathrm{e}^{3\varphi}$. However,

the trimer motion is only rotational. Hence, single trimers do not contribute to the adatom diffusion. In the following sections we do not further consider trimer oscillations or the oscillatory adatom jumps shown in Figure 1a.

3 Vacancy mechanism of tracer diffusion

In this section we will consider the situation when vacancies dominate the adatom transport. This is the case in the highly-ordered state just below the stoichiometric coverage. Once the jump probabilities of vacancies are known, we can easily describe the tracer diffusion. The tracer migration is governed by the rate equation, which in the limiting case of vanishing concentrations of vacancies, *i.e.* for $\theta \to 0.5$, is given by

$$\partial_t n^*_{\mathbf{i}} = -\sum_{\mathbf{j}} \gamma_w(\mathbf{i}-\mathbf{j})[n^*_{\mathbf{i}} n^w_{\mathbf{j}} - n^*_{\mathbf{j}} n^w_{\mathbf{i}}]. \tag{1}$$

Here the vectors $\mathbf{i}$ and $\mathbf{j}$ show the positions of adsorption sites in the filled sublattice. $n^*_{\mathbf{i}}, n^w_{\mathbf{i}}$ are the occupation numbers of site i by tagged particles or vacancies, respectively, *i.e.* $n^*_{\mathbf{i}}, n^w_{\mathbf{j}} = 0, 1$. The notation $n_{\mathbf{i}}$ refers to an ordinary particle. The sum of all occupation numbers is equal to one,

$$n^*_{\mathbf{i}} + n_{\mathbf{i}} + n^w_{\mathbf{i}} = 1,$$

i.e. double occupancy of sites is forbidden. Moreover, $\gamma_w(\mathbf{i}-\mathbf{j})$ is the probability of vacancy jumps between sites $\mathbf{i}$ and $\mathbf{j}$.

$$\gamma_w(\mathbf{i}-\mathbf{j}) = \begin{cases} \nu_0, & \text{if } |\mathbf{i}-\mathbf{j}| = \sqrt{2}a, \\ \frac{1}{2}\nu_0, & \text{if } |\mathbf{i}-\mathbf{j}| = 2a, \\ 0, & \text{if } |\mathbf{i}-\mathbf{j}| > 2a. \end{cases} \tag{2}$$

The occupation numbers are not differentiable functions of time, and it is understood that the notation $\partial_t n^*_{\mathbf{i}}$ refers to $[n^*_{\mathbf{i}}(t+\Delta t) - n^*_{\mathbf{i}}(t)]/\Delta t$ with $\Delta t \to 0$.

For low tracer concentrations tracer-tracer correlations are negligible. To obtain the diffusion coefficient in this case, it is sufficient to study the long-scale space-time asymptotic behavior of a single particle. This information is contained in the Fourier-Laplace transform of equation (1) (see [8]). For a tagged particle initially at site i ($n_{\mathbf{i}}(t=0) = \delta_{\mathbf{i},0}$) we can write

$$-\mathrm{i}\omega n^*_{\mathbf{k}\omega} = 1 - \sum_{\mathbf{j}} \gamma_w(\mathbf{i}-\mathbf{j})[n^*_{\mathbf{i}} n^w_{\mathbf{j}} - n^*_{\mathbf{j}} n^w_{\mathbf{i}}]_{\mathbf{k}\omega} \tag{3}$$

where $\mathbf{k} \to 0$ and $\omega \to 0$. The Fourier-Laplace transform of an arbitrary function $F_{\mathbf{i}}(t)$ is determined by the relation

$$F_{\mathbf{k}\omega} = \int_0^\infty \mathrm{d}t \exp(\mathrm{i}\omega t) \sum_{\mathbf{i}} \exp(-\mathrm{i}\mathbf{k}\mathbf{i}) F_{\mathbf{i}}(t). \tag{4}$$

It is convenient to perform a statistical averaging of equation (3) before any further analysis. As far as the initial position of a tagged particle is fixed, the averaging is performed over the initial distribution of vacancies only. Intuitively, it is clear that the asymptotic behavior of the tracer does not depend on the initial arrangement of the vacancies. Our procedure of averaging allows small mesoscopic fluctuations of the tracer mobility to be ignored.

Equation (1) (and Eq. (3)) describes adparticle motion *via* vacancy jumps. Its right-hand part depends on the product of two stochastic variables $n^*_{\mathbf{i}}$ and $n^w_{\mathbf{j}}$. As we see, the equation is not closed. Moreover, in general it is impossible to express the right-hand part of equation (1) as a function of $n^*_{\mathbf{i}}$ only. However, the task is simplified in the long-scale (hydrodynamic) limit ($\mathbf{k} \to 0$, $\omega \to 0$). In the following we express the part of $\left\langle n^*_{\mathbf{i}} n^w_{\mathbf{j}} \right\rangle$ which slowly varies in space and time as a function of $\langle n^*_{\mathbf{i}} \rangle$. For this purpose, we start from the evolution equation for the product $n^*_{\mathbf{i}} n^w_{\mathbf{j}}$, which can be derived in a manner similar to the derivation of equation (1). If we restrict the considerations to terms linear in vacancy concentration, we can write

$$\partial_t [n^*_{\mathbf{i}} n^w_{\mathbf{i}-\mathbf{r}}] = \gamma_w(\mathbf{r}) n^*_{\mathbf{i}-\mathbf{r}} n^w_{\mathbf{i}} - \sum_{\mathbf{s}} \gamma_w(\mathbf{s}) n^*_{\mathbf{i}} [n^w_{\mathbf{i}-\mathbf{r}} - n^w_{\mathbf{i}-\mathbf{r}+\mathbf{s}}], \tag{5}$$

where $\mathbf{r} = \mathbf{i} - \mathbf{j} \neq 0$. The vector $\mathbf{s}$ labels the NN and NNN sites of the filled sublattice. The right-hand part of equation (1) is expressed in terms of $n^*_{\mathbf{i}} n^w_{\mathbf{i}-\mathbf{r}}$ with $\mathbf{r} = \mathbf{s}$. As we see from equation (5), the value $n^*_{\mathbf{i}} n^w_{\mathbf{i}-\mathbf{r}}$ depends on two space variables $\mathbf{r}$ and $\mathbf{i}$. However, it is important to realize that equation (5) is difficult to handle since is not defined for $\mathbf{r} = 0$. A simple extension of equation (5) to include this particular point ($\mathbf{r} = 0$) can be obtained by adding the term

$$-\delta_{\mathbf{r},0} \sum_{\mathbf{s}} \gamma_w(\mathbf{s}) n^*_{\mathbf{i}} n^w_{\mathbf{i}+\mathbf{s}}$$

to the right-hand part of equation (5). Thus we can write

$$\partial_t (n^*_{\mathbf{i}} n^w_{\mathbf{i}-\mathbf{r}}) = \gamma_w(\mathbf{r}) n^*_{\mathbf{i}-\mathbf{r}} n^w_{\mathbf{i}} - \delta_{\mathbf{r},0} \sum_{\mathbf{s}} \gamma_w(\mathbf{s}) n^*_{\mathbf{i}} n^w_{\mathbf{i}+\mathbf{s}} - \sum_{\mathbf{s}} \gamma_w(\mathbf{s}) n^*_{\mathbf{i}} [n^w_{\mathbf{i}-\mathbf{r}} - n^w_{\mathbf{i}-\mathbf{r}+\mathbf{s}}], \tag{6}$$

where the vector $\mathbf{r}$ can now point to any value in the filled sublattice including the point $\mathbf{r} = 0$. Equation (6) is transformed into identity for $\mathbf{r} = 0$, which follows from $n^*_{\mathbf{i}} n^w_{\mathbf{i}-\mathbf{r}} = 0$ for $\mathbf{r} = 0$.

In a manner similar to paper [8], we introduce a tracer-vacancy correlation function

$$g^\omega_{\mathbf{k}}(\lambda) = \int_0^\infty \mathrm{d}t \exp(\mathrm{i}\omega t) \sum_{\mathbf{i},\mathbf{r}} \exp[\mathrm{i}(\lambda\mathbf{r} - \mathbf{k}\mathbf{i})] \left\langle n^*_{\mathbf{i}} [n^w_{\mathbf{i}-\mathbf{r}} - n^w] \right\rangle \tag{7}$$

with $n^w = \langle n^w_{\mathbf{i}} \rangle$. The equation of motion for $g^\omega_{\mathbf{k}}$ follows immediately from equation (6). In the limiting case of small

$\mathbf{k}$ and ω ($\mathbf{ks} \ll 1, \omega \ll \gamma_w$) this equation is given by

$$(-\mathrm{i}\omega + \omega_\lambda)[g^\omega_{\mathbf{k}}(\lambda) + n^w\langle n^*_{\mathbf{k}\omega}\rangle] = \sum_{\mathbf{s}} \gamma_w(\mathbf{s})(\mathrm{e}^{-\mathrm{i}\lambda\mathbf{s}} - 1) g^\omega_{\mathbf{k}}(\mathbf{s}) - \sum_{\mathbf{s}} \gamma_w(\mathbf{s}) \mathrm{e}^{\mathrm{i}\lambda\mathbf{s}} \mathrm{i}\mathbf{ks} n^w \langle n^*_{\mathbf{k},\omega}\rangle, \quad (8)$$

where

$$\omega_\lambda = \sum_{\mathbf{s}} \gamma_w(\mathbf{s})(1 - \mathrm{e}^{\mathrm{i}\lambda\mathbf{s}}). \quad (9)$$

The inverse Fourier transformation of equation (8) from λ to $\mathbf{r}$ variables yields a relation between the values of function $g^\omega_{\mathbf{k}}(\mathbf{r})$ with different $\mathbf{r}$, *i.e.*,

$$g^\omega_{\mathbf{k}}(\mathbf{r}) = -n^w\langle n^*_{\mathbf{k},\omega}\rangle\delta_{\mathbf{r},0} + \sum_{\mathbf{s}} \gamma_w(\mathbf{s})[g^\omega_{\mathbf{k}}(\mathbf{s}) + \mathrm{i}\mathbf{ks} n^w\langle n^*_{\mathbf{k}\omega}\rangle][P(\mathbf{r}+\mathbf{s}) - P(\mathbf{r})], \quad (10)$$

where

$$P(\mathbf{r}) = \frac{2}{N} \sum_{\lambda} \frac{\exp(-\mathrm{i}\lambda\mathbf{r})}{-\mathrm{i}\omega + \omega_\lambda}\,. \quad (11)$$

$N/2$ is the total number of sites in the filled sublattice; the sum $\sum_\lambda$ runs over $N/2$ values in the inverse sublattice. Putting $\mathbf{r}$ equal to eight different values of $\mathbf{s}$, we obtain a system of eight linear equations for the unknown quantities $g^\omega_{\mathbf{k}}(\mathbf{s})$ from equation (10). Considering the symmetry properties of the system allows further simplifications of our treatment. First of all, we can use the obvious relation $P(\mathbf{r}) = P(-\mathbf{r})$. Secondly, our purpose is to study the tracer diffusion on a square lattice. The diffusion tensor in the system with square symmetry reduces to a scalar. Therefore, it is sufficient to obtain the diffusion coefficient for any direction. Thus, without loss of generality we can consider only the case of $\mathbf{k}$ parallel to the line between the NN sites of the host lattice (see Fig. 3). As a result, the system of eight equations is reduced to only two interconnected equations. The solution is given by

$$g^\omega_{\mathbf{k}}(\mathbf{s}) = \mathrm{i}\mathbf{ks} n^w\langle n^*_{\mathbf{k},\omega}\rangle[-1 + \Delta(s)], \quad (12)$$

where

$$\Delta(\sqrt{2}a) = \frac{1 + (\nu_0/2)(P_{05} + 2P_{41})}{[1 + \nu_0 P_{03}][1 + (\nu_0/2)P_{05}] - [\nu_0 P_{14}]^2},$$

$$\Delta(2a) = \frac{1 + \nu_0(P_{03} + P_{41})}{[1 + \nu_0 P_{03}][1 + (\nu_0/2)P_{05}] - [\nu_0 P_{14}]^2}. \quad (13)$$

The quantities P_{ij} are determined by the relation $P_{ij} \equiv P(\mathbf{i}) - P(\mathbf{j})$ with the positions i, j of the lattice sites in the filled sublattice as shown in Figure 3. The values P_{ij} can be calculated numerically by employing the definitions (11, 9).

With the quantities $g^\omega_{\mathbf{k}}(\mathbf{s})$ given by equation (12) we can easily determine the tracer diffusion coefficient associated with vacancy motion. Equation (3) now takes the form

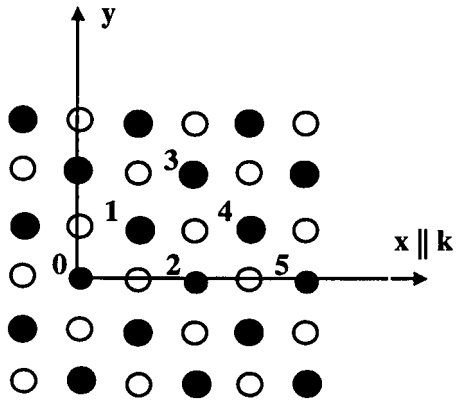

Fig. 3. Orientation of the vector $\mathbf{k}$ and the positions i, j in the notation $P_{i,j}$ (see Sects. 3 and 4).

$$-\mathrm{i}\omega\langle n^*_{\mathbf{k},\omega}\rangle = 1 - \frac{1}{2}\sum_{\mathbf{s}} \gamma_w(\mathbf{s})(\mathbf{sk})^2 n^w\langle n^*_{\mathbf{k}\omega}\rangle + \sum_{\mathbf{s}} \gamma_w(\mathbf{s})\mathrm{i}\mathbf{sk} g^\omega_{\mathbf{k}}(\mathbf{s}), \quad (14)$$

which can be transformed using equation (12) into

$$-\mathrm{i}\omega\langle n^*_{\mathbf{k},\omega}\rangle = 1 - D^*_w k^2 \langle n^*_{\mathbf{k}\omega}\rangle. \quad (15)$$

Here the tracer diffusion coefficient D^*_w represents the contribution of both sums in the right hand part of equation (14), $D^*_w = D^*_{0w} + \Delta D^*_w$. The value D^*_{0w} is given by

$$D^*_{0w} = 4D_0 n_w,$$

where $D_0 = \nu_0 a^2$. It describes the tracer diffusion coefficient if one neglects tracer-vacancy correlations (when we put the function $g^\omega_{\mathbf{k}}$ equal to zero). The quantity D^*_{0w} exactly reproduces the tracer diffusion coefficient obtained in [2], which is equal to the jump diffusion coefficient $D_{j\omega}$.

The quantity ΔD^*_w is determined by the second sum in the right-hand part of equation (14). Numerical calculations employing equations (11–14) give the value $\Delta D^*_w \approx -0.37 D^*_{0w}$. Hence, the ratio of tracer and jump diffusion coefficient is given by

$$r = D^*_w/D_{jw} = 1 + \Delta D^*_w/D^*_{0w} = 0.63,$$

i.e. tracer-vacancy correlations reduce the tracer diffusion coefficient relative to the jump diffusion coefficient. The situation is similar to the case of tracer diffusion in the Langmuir (non-interacting) lattice gas in the vicinity of full monolayer coverage, $\theta \to 1$, (see for example [8–10]). A considerable correlation between successive tracer jumps is present in that case since, after a jump of a tracer, the vacancy that promoted this jump is with certainty behind the tracer. Therefore, a backward jump of the tracer is more likely than another forward or sideward jump. As a consequence, the effective jump frequency of a tracer

is lowered. For a more detailed discussion of this "backward jump model" see the paper of Haus and Kehr [11].

The deviation of r from 1 obviously describes the tracer-defect correlation. At the same time, the correlation in tracer jumps can be described in terms of another physical quantity, namely, the correlation factor f [12,13] which is defined by the relation

$$D^* = fVa^2\Gamma, \tag{16}$$

where V is the vacancy availability factor and Γ is the adatom jump frequency. These quantities are given by

$$\Gamma = \nu_0\langle e^{\epsilon_i}(n_i/\theta)(1-n_j)\rangle/V$$

and

$$V = \langle(n_i/\theta)(1-n_j)\rangle.$$

Here the sites i and j constitute nearest neighbor sites.

We can easily see that quantities f and r are identical in the absence of interaction (when $\varphi = 0$), but differ otherwise. For the highly-ordered state considered here, we have $V \approx 1$ and $\Gamma \approx 2\nu_0$. Thus, the correlation factor is approximately given by

$$f = D_w^*/2D_0 \ll 1.$$

In other words, the correlation factor f is reduced to the normalized tracer diffusion coefficient and does not explicitly contain tracer-defect correlation effects.

There exists another definition of the correlation factor of a random walk, first given by Compaan and Haven [14]

$$f = (1 + \langle\cos\Theta\rangle)/(1 - \langle\cos\Theta\rangle), \tag{17}$$

where Θ is the angle between two successive jump vectors of the walk, and $\langle ...\rangle$ represents the average over all pairs of successive jumps. It follows from the discussion in Section 2 that oscillatory adatom jumps, shown in Figure 1a, are the most frequent event. For each pair of these jumps $\cos\Theta = -1$ and $f \to 0$ in the case of highly ordered state. This agrees well with the result obtained from the definition (16). In that case $f \propto n_w$ and $n_w \to 0$ when the ordering increases. Small values of f can also be explained by the fact that oscillatory jumps, constituting the major contribution to the jump frequency Γ, are useless in tracer diffusion.

A dramatic lowering of a the correlation factor in the vicinity of a highly ordered state was observed during Monte Carlo simulations of various lattice gas models in [1,7,15,16]. The above consideration explains this effect (see also the physical explanation given in [3]).

4 Black defect mechanism of tracer diffusion

Let us consider tracer diffusion caused by the defect motion in the empty sublattice (black defects). The black defect transport mechanism dominates for coverages slightly above the stoichiometric one, *i.e.* when excessive adatoms occupy the empty sublattice of the c(2×2) ordered state. In this case the motion of a tagged particle is more complicated than in the previous case. Figure 1b can be used to illustrate this point. Initially, the tagged particle is assumed to be in site 1. The defect jump to one of the sites 2, 3 or 4 displaces the tracer to the corresponding site with the probability equal to $\nu_0 e^{\varphi}/2 \equiv \gamma$. As a result, the tracer changes from the filled to the empty sublattice, where it forms a black defect. The next tracer jump then may occur (in the absence of another defect) with the frequency proportional to γ. Thus, we have two rate equations for this type of motion, which are given by

$$\begin{aligned}\partial_t n^*_{\mathbf{i}} &= -(3\gamma/2)\sum_{\mathbf{a}}[n^*_{\mathbf{i}} n^b_{\mathbf{i}+\mathbf{a}} - n^{b*}_{\mathbf{i}+\mathbf{a}}]\\ \partial_t n^{b*}_{\mathbf{j}} &= -6\gamma n^{b*}_{\mathbf{j}} + (\gamma/2)\sum_{\mathbf{a}\neq-\mathbf{a}_1} n^*_{\mathbf{j}+\mathbf{a}} n^b_{\mathbf{j}+\mathbf{a}+\mathbf{a}_1}.\end{aligned} \tag{18}$$

Here $n^b_{\mathbf{j}}$ and $n^{b*}_{\mathbf{j}}$ denote the defect stochastic variables; the symbol $(^*)$ represents the defect formed by the tagged particle. The vectors $\mathbf{a}$ and $\mathbf{a}_m$ run over NN sites of the host lattice ($|\mathbf{a}|$, $|\mathbf{a}_m| = a$). The system (18) is not closed. It should be completed by the evolution equation for the pair stochastic function $n^*_{\mathbf{i}} n^b_{\mathbf{j}}$. This equation is given by

$$\begin{aligned}\partial_t(n^*_{\mathbf{i}} n^b_{\mathbf{j}}) = \frac{\gamma}{2}\sum_{\mathbf{a}\neq-\mathbf{a}_1}\delta_{\mathbf{i}-\mathbf{j},\mathbf{a}_1}(n^{b*}_{\mathbf{i}+\mathbf{a}} - n^*_{\mathbf{i}} n^b_{\mathbf{i}+\mathbf{a}})\\ -\frac{\gamma}{2}\sum_{\mathbf{a}\neq-\mathbf{a}_1} n^*_{\mathbf{i}}(n^b_{\mathbf{j}} - n^{b*}_{\mathbf{j}+\mathbf{a}+\mathbf{a}_1}),\end{aligned} \tag{19}$$

where the vectors $\mathbf{i}$ and $\mathbf{j}$ belong to different sublattices.

As before, it is convenient to introduce a function describing correlations in the tracer-black defect motion. This function has the form

$$G_{\mathbf{i}}(\mathbf{r},t) = \langle n^*_{\mathbf{i}}(n^b_{\mathbf{i}-\mathbf{r}} - n^b)\rangle. \tag{20}$$

Employing equations (18, 19) we easily obtain an equation for the Fourier-Laplace transform of G. It is given by

$$\begin{aligned}(-\mathrm{i}\omega + \omega_\lambda)G^\omega_{\mathbf{k}}(\lambda) = \frac{\gamma}{2}\sum_{\mathbf{a}}[(e^{\mathrm{i}\lambda\mathbf{a}} - \frac{1}{4}\sum_{\mathbf{a}_1} e^{\mathrm{i}\lambda\mathbf{a}_1})G^\omega_{\mathbf{k}}(\mathbf{a})\\ + \mathrm{i}\mathbf{k}\mathbf{a}e^{\mathrm{i}\lambda\mathbf{a}} n^b\langle n^*_{\mathbf{k}\omega}\rangle],\end{aligned} \tag{21}$$

where

$$\omega_\lambda = \frac{\gamma}{2}\sum_{\mathbf{a},\mathbf{a}_1}[1 - e^{\mathrm{i}\lambda(\mathbf{a}+\mathbf{a}_1)}].$$

Equation (21) yields a system of four interconnected equations for the functions $G^\omega_{\mathbf{k}}(\mathbf{a})$,

$$\begin{aligned}G^\omega_{\mathbf{k}}(\mathbf{a}) = \frac{\gamma}{2}\sum_{\mathbf{a}_1}\big[P(\mathbf{a}-\mathbf{a}_1) - \frac{1}{4}\sum_{\mathbf{a}_2} P(\mathbf{a}-\mathbf{a}_2)\big]\big[G^\omega_{\mathbf{k}}(\mathbf{a}_1)\\ + \mathrm{i}\mathbf{k}\mathbf{a}_1 n^b\langle n^*_{\mathbf{k}\omega}\rangle\big].\end{aligned} \tag{22}$$

The quantity $P(\mathbf{r})$ is defined by equation (11). The solution of equation (22) is very simple, *i.e.*,

$$G^\omega_{\mathbf{k}}(\mathbf{a}) = \mathrm{i}\mathbf{k}\mathbf{a}n^b n^*_{\mathbf{k},\omega}\Delta, \tag{23}$$

where $\Delta = \gamma P_{02}/(2-\gamma P_{02})$. The index 02 denotes the sites 0 and 2 as shown in Figure 3.

With the functions $G^{\omega}_{\mathbf{k}}(\mathbf{a})$ it is possible to find the tracer diffusion coefficient. Considering the system of equations (18) and the definition (20), the values $\langle n^*_{\mathbf{k}\omega}\rangle$ and $G^{\omega}_{\mathbf{k}}(\mathbf{a})$ are related by

$$-\mathrm{i}\omega\langle n^*_{\mathbf{k}\omega} + n^{*b}_{\mathbf{k},\omega}\rangle = 1 - 3\gamma a^2 k^2 n^b \langle n^*_{\mathbf{k}\omega}\rangle - \frac{\gamma}{2}\sum_{\mathbf{a}} \mathbf{k}\mathbf{a} G^{\omega}_{\mathbf{k}}(\mathbf{a}) \tag{24}$$

The second term in the brackets of the left-hand part can be neglected. Its value is of the order of n^b, *i.e.* much smaller compared to the remaining terms of equation (24). Using equation (23), equation (24) is transformed to

$$-\mathrm{i}\omega\langle n^*_{\mathbf{k}\omega}\rangle = 1 - 3D_0 \mathrm{e}^{\varphi} n^b (1-\Delta/3) k^2 \langle n^*_{\mathbf{k},\omega}\rangle. \tag{25}$$

Thus the tracer diffusion coefficient D^*_b is given by

$$D^*_b = 3D_0 \mathrm{e}^{\varphi} n^b (1-\Delta/3), \tag{26}$$

where the second term in the brackets $(\Delta/3)$ accounts for the contribution of $G^{\omega}_{\mathbf{k}}(\mathbf{r})$ and thus represents the effect of tracer-defect correlations. The numerical calculations yield $\Delta/3 \approx 0.033$. Hence, we have $D^*_b = 2.9 D_0 \mathrm{e}^{\varphi} n^b$, which is very similar to our earlier result $D^*_{0b} = 3D_0 \mathrm{e}^{\varphi} n^b$ [2,4]. With $D_{jb} = 4D_0 n^b$ as jump diffusion coefficient the ratio $r = D^*_b/D_{jb}$ is $\approx 3/4$ as before.

5 Black dimer mechanism of tracer diffusion

The theoretical value of r and corresponding Monte Carlo data do not well agree for coverages with prevailing black dimer transport [2]. Therefore, it is important to account for correlation effects in the motion of dimers. It is quite obvious that the concerted motion of defects and tagged particles is the most complex problem considered in this paper. Figure 2b illustrates the correlated jumps of dimers and tracer particles. Initially, the tagged particle is in site 3 of the filled sublattice, and the dimer is formed by the defects in sites 1 and 2 of the empty sublattice. Two possible successive jumps of the dimer to 1-4 and 1-6 positions are shown in Figure 2b. These jumps are accompanied by tracer displacements from site 3 to the sites 4 and 5. The tracer becomes a constituent of the 1-4 dimer after its jump from site 3 to site 4. The picture is very similar to the case of black defect motion where the tracer in the empty sublattice becomes the black defect.

The general scheme of the theoretical description of this particular case is similar to the previous cases. It is convenient to proceed from the evolution of the total occupancy of site i and its NN minima, namely,

$$n^*_{\mathbf{i}} + \frac{1}{4}\sum_{\mathbf{a}} n^*_{\mathbf{i}+\mathbf{a}}.$$

Here we assume that site i belongs to a filled sublattice. Before writing the rate equation, we introduce the notation for the dimer variables: $n^{\mathbf{j}}_{\mathbf{i}}$ denotes the dimer formed by the pair of defects in the sites i and j of the empty sublattice ($|\mathbf{i}-\mathbf{j}| = \sqrt{2}a$ or $2a$); $n^{\mathbf{j}}_{\mathbf{i}*}$ means that the defect in the site i is formed by a tagged particle.

Thus the rate equation is given by

$$\begin{aligned}\partial_t\Big(n^*_{\mathbf{i}} + \frac{1}{4}\sum_{\mathbf{a}} n^*_{\mathbf{i}+\mathbf{a}}\Big) = {} & \frac{3}{2}\Gamma\sum\big(n^{\mathbf{i}+\mathbf{a}_1}_{\mathbf{i}+\mathbf{a}*} - n^*_{\mathbf{i}} n^{\mathbf{i}+\mathbf{a}_1}_{\mathbf{i}+\mathbf{a}}\big) \\ & + \frac{\Gamma}{4}\sum\big(n^*_{\mathbf{i}+\mathbf{a}+\mathbf{a}_1} n^{\mathbf{i}+\mathbf{a}+\mathbf{a}_1+\mathbf{a}_3}_{\mathbf{i}+\mathbf{a}+\mathbf{a}_1+\mathbf{a}_2} \\ & - n^{\mathbf{i}+\mathbf{a}+\mathbf{a}_1+\mathbf{a}_2}_{\mathbf{i}+\mathbf{a}*}\big).\end{aligned} \tag{27}$$

The first sum in the right-hand part runs over the vectors $\mathbf{a}, \mathbf{a}_1$ excluding the terms with $\mathbf{a} = \mathbf{a}_1$. The second sum runs over the vectors $\mathbf{a}, \mathbf{a}_1$, $\mathbf{a}_2$, $\mathbf{a}_3$ excluding the terms with $\mathbf{a}, \mathbf{a}_2$, $\mathbf{a}_3 = -\mathbf{a}_1$ and $\mathbf{a}_2 = \mathbf{a}_3$.

Similar to the situations studied in Sections 3 and 4, the right-hand part of the rate equation depends on the products of stochastic variables. It is useful to simplify the treatment, for instance by summing up over the vectors $\mathbf{a}_i$ in (27). For this purpose, we will perform the Fourier-Laplace transformation of equation (27) assuming that the wave vector is directed along one of the vectors $\mathbf{a}$: $\mathbf{k}\|\mathbf{a}\|\mathbf{x}$ (see Fig. 3). As in the previous sections, we will treat the case $\mathbf{k} \to \mathbf{0}$. Then equation (27) is transformed into

$$\begin{aligned}-\mathrm{i}\omega\langle n^*_{\mathbf{k}\omega}\rangle = {} & 1 - 12\Gamma(ka)^2 n_d \langle n^*_{\mathbf{k}\omega}\rangle + \Gamma ka\{-ka[G(\mathbf{a}_{\|}, -\mathbf{a}_{\|}) \\ & + 3G(\mathbf{a}_{\perp}, -\mathbf{a}_{\perp}) + 4G(\mathbf{a}_{\|}, \mathbf{a}_{\perp}) + 4G(-\mathbf{a}_{\|}, \mathbf{a}_{\perp})] \\ & + 4\mathrm{i}[G(\mathbf{a}_{\|}, \mathbf{a}_{\perp}) - G(-\mathbf{a}_{\|}, \mathbf{a}_{\perp})] + 2\mathrm{i}[-d(2\mathbf{a}_{\|}) \\ & + d(-2\mathbf{a}_{\|}) - 2d(\mathbf{a}_{\|} + \mathbf{a}_{\perp}) + 2d(-\mathbf{a}_{\|} + \mathbf{a}_{\perp})]\},\end{aligned} \tag{28}$$

where the vectors $\mathbf{a}_{\|}$ and $\mathbf{a}_{\perp}$ are directed along the $\mathbf{x}$ and $\mathbf{y}$ axes, respectively ($|\mathbf{a}_{\|,\perp}| = a$). The correlation functions $G(\mathbf{a}, \mathbf{a}_1)$ and $d(\mathbf{a} + \mathbf{a}_1)$ are defined by the relations

$$\begin{aligned}G(\mathbf{a}, \mathbf{a}_1) &= \int_0^{\infty} \mathrm{d}t \sum_{\mathbf{i}} \mathrm{e}^{\mathrm{i}\omega t - \mathrm{i}\mathbf{k}\mathbf{i}} \Big\langle n^*_{\mathbf{i}}\big(n^{\mathbf{i}+\mathbf{a}_1}_{\mathbf{i}+\mathbf{a}} - n_d\big)\Big\rangle \\ d(\mathbf{a} + \mathbf{a}_1) &= \int_0^{\infty} \mathrm{d}t \sum_{\mathbf{i}} \mathrm{e}^{\mathrm{i}\omega t - \mathrm{i}\mathbf{k}\mathbf{i}} \Big\langle n^{\mathbf{i}+\mathbf{a}+\mathbf{a}_1}_{\mathbf{i}*} - n^*_{\mathbf{i}} n_d\Big\rangle,\end{aligned} \tag{29}$$

where

$$n_d \equiv \Big\langle n^{\mathbf{i}+\mathbf{a}_1}_{\mathbf{i}+\mathbf{a}}\Big\rangle = (n^b)^2.$$

For the sake of brevity, we have not indicated the dependencies of G and d on $\mathbf{k}$ and ω in equations (28, 29).

The evolution of $\langle n^*_{\mathbf{k}\omega}\rangle$ is determined by the correlation functions $G(\mathbf{a}, \mathbf{a}_1)$ and $d(\mathbf{a} + \mathbf{a}_1)$. However, only terms linear and quadratic in ka enter the right-hand part of equation (28). Therefore, it is sufficient to obtain the terms $G(\mathbf{a}, \mathbf{a}_1)$ and $d(\mathbf{a}+\mathbf{a}_1)$ of zeroth and first order in ka. These observations considerably simplify our task.

The rate equations for the stochastic pair variables are given by

$$\begin{aligned}\partial_t(n_{\mathbf{i}}^* n_{\mathbf{l}}^{\mathbf{l+a+a}_1}) = \Gamma(1-\frac{1}{2}\delta_{\mathbf{a},\mathbf{a}_1})\{&-8n_{\mathbf{i}}^* n_{\mathbf{l}}^{\mathbf{l+a+a}_1}\\ &+\sum_{\mathbf{a}_2\neq-\mathbf{a},\mathbf{a}_1}[n_{\mathbf{i}}^*(n_{\mathbf{l}}^{\mathbf{l+a+a}_2}+n_{\mathbf{l}}^{\mathbf{l+a}_1-\mathbf{a}_2}\\ &+n_{\mathbf{l+a}_1-\mathbf{a}_2}^{\mathbf{l+a+a}_1}+n_{\mathbf{l+a+a}_2}^{\mathbf{l+a+a}_1})\\ &+\delta_{\mathbf{l},\mathbf{i}-\mathbf{a}}(n_{\mathbf{i+a}_2*}^{\mathbf{i+a}_1}+n_{\mathbf{i+a}_2*}^{\mathbf{i}-\mathbf{a}}-n_{\mathbf{i}}^* n_{\mathbf{i}-\mathbf{a}}^{\mathbf{i+a}_2}\\ &-n_{\mathbf{i}}^* n_{\mathbf{i+a}_2}^{\mathbf{i+a}_1})+\mathbf{a}\longleftrightarrow\mathbf{a}_1]\}\\ \partial_t n_{\mathbf{i}-\mathbf{a}_1*}^{\mathbf{i}-\mathbf{a}} = \Gamma(1-\frac{1}{2}\delta_{\mathbf{a},-\mathbf{a}_1})\{&-8n_{\mathbf{i}-\mathbf{a}_1*}^{\mathbf{i}-\mathbf{a}}\\ &+\sum_{\mathbf{a}_2\neq\mathbf{a},\mathbf{a}_1}[n_{\mathbf{i}-\mathbf{a}_1*}^{\mathbf{i}-\mathbf{a}-\mathbf{a}_1+\mathbf{a}_2}+n_{\mathbf{i}-\mathbf{a}_1*}^{\mathbf{i}-\mathbf{a}_2}+n_{\mathbf{i}}^* n_{\mathbf{i}-\mathbf{a}_2}^{\mathbf{i}-\mathbf{a}}\\ &+n_{\mathbf{i}-\mathbf{a}-\mathbf{a}_1}^* n_{\mathbf{i}-\mathbf{a}-\mathbf{a}_1+\mathbf{a}_2}^{\mathbf{i}-\mathbf{a}}]. \qquad (30)\end{aligned}$$

The notation $\mathbf{a}\longleftrightarrow\mathbf{a}_1$ in equation (30) implies the term equal to the previous one with the vectors $\mathbf{a}$ and $\mathbf{a}_1$ being interchanged.

Our theory deals with the complicated three-particle kinetics on 2D discrete lattice with the peculiar condition that a pair of defects are separated by the distances $\sqrt{2}a, 2a$ to form a black defect dimer, and each pair of different particles (defects and tracers) are allowed at arbitrary distances (including double occupancy of the same site). This situation can be treated in a manner similar to the previous cases. After statistical averaging and Fourier-Laplace transforming, equation (30) reduces to a system of linear equations with respect to the pair correlation functions. These linear equations are similar to equations (8, 21) discussed earlier. A straightforward solution of the problem employing double Fourier transformations from the real space domain to $\mathbf{k}, \lambda$ variables is too tedious. Therefore, we will restrict the considerations to an approximate solution taking into account tracer-dimer correlations only for a few specific situations, for instance (i) when the tracer and both defects are NN, or (ii) when the tracer is a constituent of the dimer. The approximation assumes that

$$\langle n_{\mathbf{i}}^* n_{\mathbf{l}}^{\mathbf{l+s}}\rangle \approx \langle n_{\mathbf{i}}^*\rangle\langle n_{\mathbf{l}}^{\mathbf{l+s}}\rangle \equiv \langle n_{\mathbf{i}}^*\rangle n^d, \qquad (31)$$

if at least one of the two distances $|\mathbf{i}-\mathbf{l}|, |\mathbf{i}-\mathbf{l}-\mathbf{s}|$ is longer than $2a$ (this is the case, for example, when the black dimer is in sites 2 and 7 and the tracer is in site 3, see Fig. 2b). Thus, equation (31) corresponds to the short-range correlation approximation.

The approximation given by equation (31) is justified by the underlying physical picture. The probabilities of tracer displacements due to the dimer jumps from the positions 1-2, 1-4 and 1-6 shown in Figure 2b are equal to either one or one half. We can see strong tracer-dimer correlations here. In contrast, if the tracer is not a dimer constituent or if at least one of the defects is not a NN of the tracer, then the probability of a concerted tracer-dimer jump is equal to zero. Obviously, the dimer can "find" the tracer in some jumps, thus providing more distant correlation effects (or memory effects). Nevertheless, it seems that the contribution of the long-range correlations is less significant compared to the short-range correlations.

Approximation (31) allows us to obtain a system of interconnected equations for the values G and d. These equations are derived with regard for equation (30). We can write

$$\begin{aligned}&8\left(1-\frac{1}{2}\delta_{\mathbf{a},-\mathbf{a}_1}\right)G(\mathbf{a},\mathbf{a}_1)\\ &-\sum_{\mathbf{a}_2\neq\mathbf{a},\mathbf{a}_1}[d(\mathbf{a}-\mathbf{a}_2)+d(\mathbf{a}_1-\mathbf{a}_2)] = 2\sum_{\mathbf{a}_2\neq\mathbf{a},\mathbf{a}_1}\mathrm{i}\mathbf{k}\mathbf{a}_2 n_d\langle n_{\mathbf{k}\omega}^*\rangle\end{aligned}$$

$$\begin{aligned}&8d(\mathbf{a}+\mathbf{a}_1)-\sum_{\mathbf{a}_2\neq-\mathbf{a},\mathbf{a}_1}[d(\mathbf{a}+\mathbf{a}_2)+d(\mathbf{a}_1-\mathbf{a}_2)\\ &+G(\mathbf{a},-\mathbf{a}_2)+G(\mathbf{a}_1,\mathbf{a}_2)] = 2\mathrm{i}\mathbf{k}(\mathbf{a}+\mathbf{a}_1)n_d\langle n_{\mathbf{k}\omega}^*\rangle. \qquad (32)\end{aligned}$$

For our specific choice of the direction of $\mathbf{k}$, equations (32) reduce to only nine interconnected equations. Substituting the solutions of this system in equation (28), we get

$$-\mathrm{i}\omega\langle n_{\mathbf{k}\omega}^*\rangle = 1 - D_{0d}^*(1-\Delta_{\mathrm{corr}})k^2\langle n_{\mathbf{k}\omega}^* 2\rangle, \qquad (33)$$

where $D_{0d}^* = 4D_0(\mathrm{e}^{\varphi}n^b)^2$ is the value of the tracer diffusion coefficient obtained in [2] ignoring tracer-dimer correlations (when $G(\mathbf{a},\mathbf{a}_1) = d(\mathbf{a}-\mathbf{a}_1) = 0$). The quantity Δ_{corr} linearly depends on the functions G and d, and accounts for the tracer-dimer correlations. Numerical calculations yield $\Delta_{\mathrm{corr}} \approx 0.47$. Hence, it follows from equation (33) that the tracer diffusion coefficient D_d^* is equal to $D_d^* \approx 2.12D_0(\mathrm{e}^{\varphi}n^b)^2$. In reference [2] the jump diffusion coefficient, associated with dimer motion, is obtained as $D_{\mathrm{j}d} = \frac{16}{3}D_0(\mathrm{e}^{\varphi}n^b)^2$. As we see, the coefficient r is equal to $r = (D_d^*/D_{\mathrm{j}d}) \approx 0.4$ in this case. This value is in much better agreement with the results of computer simulations than $r = 0.75$ obtained in [2].

6 Comparison of theory and Monte Carlo simulation data

The complete expression for the tracer diffusion coefficient, $D^* = D_w^* + D_b^* + D_d^*$, is given by

$$D^* = 4D_0[0.63n_w + 0.72n_b\mathrm{e}^{\varphi} + 0.53(n_b\mathrm{e}^{\varphi})^2]. \qquad (34)$$

The average occupation numbers of vacancies and black defects, $n_{b,w}$, were obtained in [2,4] as by

$$n_{b,w} = \pm(\theta-1/2) + \sqrt{(\theta-1/2)^2+\mathrm{e}^{-4\varphi}}. \qquad (35)$$

The dependence $D^*(\theta)$ is qualitatively very similar to that of the jump diffusion coefficient $D_{\mathrm{j}}(\theta)$,

$$D_{\mathrm{j}} = 4D_0[n_w + n_b\mathrm{e}^{\varphi} + (4/3)(n_b\mathrm{e}^{\varphi})^2], \qquad (36)$$

which was obtained already in reference [2]. Both functions are shown in Figure 4 for two characteristic temperatures, $T = 0.5T_{\mathrm{c}}$ and $T = 0.7T_{\mathrm{c}}$, *i.e.* well below T_{c}.

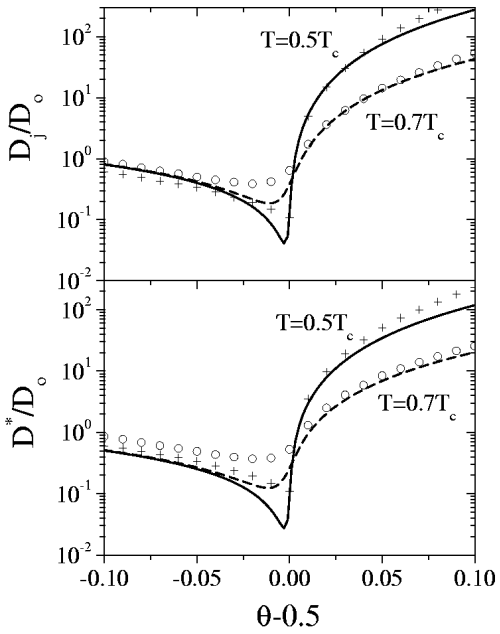

Fig. 4. Coverage dependence of tracer and jump diffusion coefficients (D^* and $D_{\rm j}$, respectively). Symbols show the results of MC simulation. Dashed lines and symbols (°) correspond to temperature $0.7T_{\rm c}$ ($\varphi = 2.52$); solid lines and symbols (+) are for $T = 0,5T_{\rm c}$ ($\varphi = 3.53$).

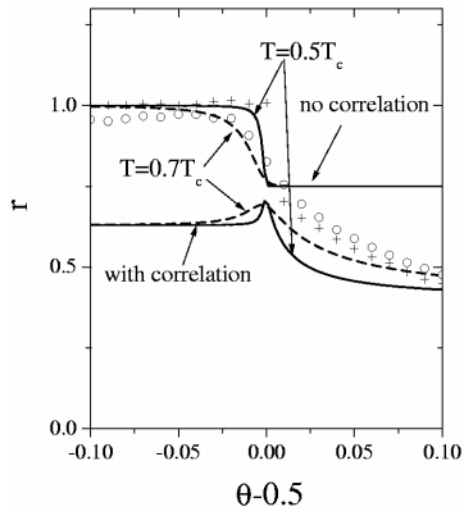

Fig. 5. The ratio of tracer and jump diffusion coefficients. The results of previous theory [2] are shown by two upper curves. The two lower curves are plotted with the use of the expression (34). Notations as in [2].

The agreement between theory (lines) and Monte Carlo [17] data (symbols) is good, though not perfect. Deviations are most prominent at the pathological coverage $\theta = 0.5$, but also for $\theta \gg 0.5$, $T = 0.5T_{\rm c}$ and, especially in the case of D^*, for $\theta \ll 0.5$.

Despite the formal similarity between the corresponding functional dependencies of D^* and D_j, their numerical values are quantitatively different. In order to emphasize the differences, we present their ratio r in Figure 5. Exact results for r are available from the literature for the limiting cases $\theta \to 0, 1$ for the non-interacting lattice gas. For $\theta \to 1$ Montet, Nakazato and Kitahara give $r \approx 0.47$ [9,10]. It is probably interesting to recall that the vacancy mechanism of tracer diffusion (considered in Sect. 3), which dominates tracer diffusion for coverages $\theta < 0.5$, is very similar to the case $\theta \to 1$ of the non-interacting lattice gas. However, the most obvious difference is that in the former case the white defect can jump to NN *and* NNN sites as well. The additional possibility of vacancy jumps to NNN sites lowers the probability of backward jumps of the tracer after each displacement and this, in turn, lowers the correlation effect relative to the situation for the non-interacting lattice gas and $\theta \to 1$. Hence, it is reasonable to assume that the possibility of white defect NNN jumps largely accounts for the calculated value of $r = 0.63$ compared to the $\theta \to 1$ limit of $r \approx 0.47$ in the non-interacting lattice gas.

The MC simulation yields $r \approx 1$ in the range of vacancy transport mechanism (for $\theta < 0.5$). In general, this value is typical for systems without any correlation. It is quite obvious that the Monte Carlo data agree much better with the tracer diffusion coefficient D_0^*

$$D_0^* = 4D_0 \left[n_w + 0.75 n_b {\rm e}^{\varphi} + (n_b {\rm e}^{\varphi})^2\right] \qquad (37)$$

obtained under the assumption of negligible tracer-defect correlation in [2]. To elucidate the evident disagreement between theory and MC simulation, a series of very time-expensive MC studies is required because of the low mobility of vacancies in this regime.

The pathological point $\theta = 0.5$ has to be discussed separately. It follows from equation (35) that the number of defects is lowered exponentially upon increasing the interaction parameter (as ${\rm e}^{-2\varphi}$). The available defects originate only from thermal pair generation processes. The corresponding generation term obtained in [2] depends on ${\rm e}^{-3\varphi}$. For the computer algorithm employed here (see details in [3]) the required computer time, which ensures many generation events on the whole surface, grows according to ${\rm e}^{6\varphi}$. To overcome this problem of freezing of adatom motion at $\theta = 0.5$ rather sophisticated algorithms have been developed recently, for instance the one described by Bulnes *et al.* [19]. The values of D^* obtained in [19] agree well with our theoretical data for $\theta = 0.5$.

Next we will discuss the behavior of the tracer diffusion coefficient in the case of the black defect transport mechanism (for $\theta > 0.5$). One has to take into account the observation that the tagged particle modifies the sublattices after each jump. The tagged particle in the empty sublattice itself forms a defect which can jump in any direction with equal probabilities irrespective of the previous jump. This weakens the memory of the system concerning the preceding first tracer jump and lowers the value of the tracer-black defect correlation function. The contribution of this correlation function to the overall tracer diffusion coefficient amounts to about 3 percent only. However, this does not mean that the correlation effect in the adatom transport is weak. Each jump of the black defect is the result of two strongly correlated jumps of different adatoms.

The value $r = \frac{3}{4}$ obtained and explained in our previous paper just reflects this type of correlation (the correlation of two successive adatom jumps). The physical explanation for $r = \frac{3}{4}$ given in reference [2] does not employ the concept of the tracer-black defect correlation. In general, the non-zero value of the tracer-defect correlation function implies the presence of high-level correlations in the adatom motion: the correlation of at least four adatom jumps which occur in the course of two defect jumps. Our study shows that such correlations do not contribute considerably in the case of the black defect mechanism.

The various reasons discussed in the preceding paragraph explain the lowering of r if black dimer transport replaces single defect transport. In this case, the tracer changes the sublattices after each jump, too. This factor by itself results in r equal to $\frac{3}{4}$ (as in the simplified version of the theory in [2]). Further lowering of r from 0.75 to 0.4 is due to the effect of tracer-dimer correlations. This pronounced correlation effect can be easily explained from geometric consideration (see Fig. 2b). After jumping from site 3 to site 4, the tracer becomes a constituent of the 1-4 dimer. The next dimer jump can displace the tracer to site 5 (in the direction perpendicular to the initial displacement) or to site 3 (in the backward direction), but not along the 3-4 direction. Thus, we see an evident tendency of returning to the initial state. This is in contrast to the case of the black defect mechanism when the black defect tracer can jump to each NN site with the same probability. The prevailing tendency of jumping to the initial state means that the tracer effective jump frequency is lowered and, of course, this results in the lowering of the diffusion coefficient. A similar analysis can be applied to the tracer which is a constituent of a NNN dimer. The tracer-dimer correlations are of great importance here, too. The MC simulation provides evidence supporting this qualitative consideration and the results of the theory in the coverage range of dominating dimer transport.

7 Summary

We have presented an analytical study of adatom migration of repulsively interacting adatoms on the two-dimensional square lattice. The theory developed here and in paper [2], is applicable for the highly-ordered state only. The analytical expression for the tracer diffusion coefficient contains information about correlation (memory) effects in the adparticle motion. We have compared the results of the theory with corresponding Monte Carlo results. Both approaches are complementary to each other, since the special case $\theta = 0.5$ which is difficult to treat *via* MC is the most appropriate for the theoretical treatment. Each of them has specific advantages useful for the comprehensive study of diffusion in highly-ordered lattice-gas systems.

The authors would like to acknowledge stimulating discussions with P. Argyrakis, V. Bondarenko, and S. Luk'yanetz. This work was financially supported by the Ukrainian State Fund of Fundamental Research (Project #2.4/558) and by the International Association for the promotion of cooperation with scientists from the New Independent States of the former Soviet Union INTAS (#96-0533).

References

1. R. Kutner, K. Binder, K.W. Kehr, Phys. Rev. B **28**, 1846 (1983).
2. A.A. Chumak, C. Uebing, Eur. Phys. B **9**, 323 (1999).
3. C. Uebing, R. Gomer, J. Chem. Phys. **95**, 7626 (1991); **95**, 7636 (1991); **95**, 7641 (1991); **95**, 7648 (1991).
4. A.A. Chumak, C. Uebing, Ukrainskij Fizychnij Zhurnal. **44**, 180 (1999).
5. A.A. Chumak, A.A. Tarasenko, Surf. Sci. **91**, 694 (1980).
6. V.P. Zhdanov, Surf. Sci. Lett. **149**, L13 (1985).
7. I. Vattulainen, J. Merikoski, T. Ala-Nisilla, S.C. Ying, Phys. Rev. B **57**, 1896 (1998).
8. R.A. Takhir-Kelly, R.J. Elliott, Phys. Rev. B. **27**, 844 (1983).
9. K. Nakazato, K. Kitahara, Progr. Theor. Phys. **64**, 2261 (1980).
10. G.L. Montet, Phys. Rev. B. **7**, 650 (1973).
11. J.W. Haus, K.W. Kehr, Phys. Rep. **150**, 263 (1987).
12. G.E. Murch, R.J. Thorn, J. Phys. Chem. Solids **38**, 789 (1977).
13. K.W. Kehr, K. Binder, Simulation of Diffusion in Lattice Gases and Related Kinetic Phenomena, in *Application of Monte Carlo Method in Statistical Physics*, edited by K. Binder (Springer-Verlag, Berlin, 1984).
14. K. Compaan, Y. Haven, Trans. Faraday Soc. **52**, 786 (1956).
15. See AIP document no. PAPS JCPSA-95-7626-9.
16. A. Sadiq, K. Binder, Surf. Sci. **128**, 350 (1983).
17. Technical details of the Monte Carlo simulations and a description of our algorithm are given in [18] and will not be repeated here. In the present work a fully parallelized version of our algorithm was run either on the Cray T3E (LC672-128) operated by the Max-Planck community in Garching/Germany or on a homemade parallel machine consisting of 10 low-cost LINUX PC's (Celeron 466MHz).
18. A.A. Tarasenko, F. Nieto, C. Uebing, Defect and Diffusion Forum **162-163**, 59 (1998).
19. F.M. Bulnes, V.D. Pereyra, J.L. Riccardo, Phys. Rev. E. **58**, 86 (1998).